

Intelligent Speed Control of Brushless DC Motor Using a Hybrid PID-ANN Controller: Design, Simulation, and Performance EvaluationKavish G. Gaurkhede¹, Dr. Umesh E. Hiwase²^{1,2}*Department of Electrical Engineering, Priyadarshini College of Engineering, Nagpur, India*

ORCID: 0009-0000-1756-5858 (K.G. Gaurkhede), 0000-0002-9763-1049 (U.E. Hiwase)

Abstract

BLDC motors have become increasingly popular across industries thanks to their high efficiency, strong torque output relative to size, low upkeep, and long service life. Yet controlling their speed accurately when loads keep changing is still a tough problem. Conventional PID controllers are widely used for their simplicity, but they often struggle with unpredictable motor behaviour, sudden load shifts, and system nonlinearities. This study explores a hybrid PID-ANN controller designed to improve BLDC motor speed regulation. The core idea is straightforward — an artificial neural network continuously adjusts the PID gains (K_p , K_i , K_d) in real time, helping the system adapt to varying conditions on the fly. The entire drive system, including the inverter, Hall-effect sensors, and back-EMF feedback, was modelled and tested in MATLAB/Simulink. Performance was evaluated across step response, load rejection, speed tracking, and torque ripple scenarios. When compared against a standard PID and a standalone ANN controller, the hybrid approach delivered notably better results, roughly 45.8% faster rise time, 48.6% quicker settling, 75.3% less overshoot, and 80% improvement in steady-state accuracy. These findings suggest that blending neural networks with traditional control methods holds real promise for advanced motor drives.

Keywords—BLDC motor, PID controller, Artificial Neural Network, hybrid PID-ANN, speed control, intelligent control, motor drive systems.

I. INTRODUCTION

Electric motors form the backbone of modern industrial automation, robotics, electric vehicle propulsion, and consumer electronics. Among the diverse family of electric machines, induction motors have historically dominated the industrial landscape due to their rugged construction, low cost, and reliable operation. Nevertheless, the inherent limitations of induction motors—particularly their reliance on slip for torque production, nonlinear speed-torque characteristics, and relatively lower efficiency at partial loads—have motivated engineers and researchers to explore superior alternatives.

Brushless DC motors have emerged as a compelling substitute, offering a constellation of advantages that make them well-suited for precision applications. Unlike their brushed counterparts, BLDC motors eliminate the mechanical commutator and carbon brushes, thereby drastically reducing wear, acoustic noise, and electromagnetic interference. The use of permanent magnets on the rotor, combined with electronically controlled stator windings, enables flat torque characteristics across a wide speed range, high power density, and energy-efficient operation. These attributes have propelled BLDC motors into applications ranging from electric vehicles and aerospace actuators to medical devices, CNC machinery, and household appliances.

Despite these inherent merits, precise speed control of BLDC motors under varying load conditions, temperature fluctuations, and parametric uncertainties remains a non-trivial engineering problem. The conventional approach of employing a fixed-gain PID controller, while widely adopted owing to its simplicity and ease of implementation, exhibits well-documented shortcomings when applied to nonlinear, time-varying systems. Specifically, a PID controller tuned for one operating point may produce unacceptable overshoot, sluggish settling, or significant steady-state error when the motor encounters a sudden torque disturbance or a change in reference speed. The limitations of conventional PID controllers have catalyzed a vibrant research landscape in intelligent and adaptive control strategies. Fuzzy logic controllers, genetic algorithm-optimized PIDs, particle swarm optimization (PSO)-based tuning, sliding mode controllers, and model predictive control have all been explored with varying degrees of success [1]–[6]. Among these, artificial neural networks stand out for their universal function approximation capability, capacity to learn complex nonlinear mappings from data, and ability to adapt in real time without requiring an explicit mathematical model of the plant. This paper proposes a hybrid PID-ANN controller that synergistically combines the structural simplicity and stability guarantees of the PID framework with the adaptive intelligence of neural networks. The ANN component continuously monitors the error dynamics of the system and adjusts the PID gains in real time, effectively creating a self-tuning controller that can handle nonlinearities, load disturbances, and parameter variations with minimal human intervention. The entire system is modeled and simulated in MATLAB/Simulink, and a rigorous performance comparison is conducted against conventional PID and standalone ANN controllers.

The remainder of this paper is organized as follows: Section II provides a comprehensive overview of BLDC motor construction and operating principles. Section III presents a comparative analysis of BLDC motors with brushed DC motors and induction motors. Section IV details the mathematical modeling of the BLDC motor. Section V describes the design of PID, ANN, and hybrid PID-ANN controllers. Section VI presents the MATLAB/Simulink simulation environment. Section VII discusses simulation results and comparative performance analysis. Section VIII draws conclusions and suggests future research directions.

II. BLDC MOTOR: CONSTRUCTION AND OPERATING PRINCIPLES

A BLDC motor is fundamentally a permanent magnet synchronous machine that operates on direct current through an electronic commutation circuit. The motor consists of two primary components: a stationary stator carrying three-phase concentrated or distributed windings, and a rotor embedded with high-energy permanent magnets—typically neodymium iron boron (NdFeB) or samarium cobalt (SmCo). The electronic commutation replaces the mechanical brushes and commutator found in traditional DC motors, using solid-state semiconductor switches (typically MOSFETs or IGBTs) arranged in a three-phase inverter bridge configuration. The commutation sequence is governed by the rotor's angular position, which is detected either through discrete Hall-effect sensors mounted at 120-degree electrical intervals around the stator, or through sensorless techniques that estimate the rotor position from the back electromotive force (back-EMF) waveforms induced in the unenergized phase windings. In a three-phase BLDC motor, two of the three phases are energized at any given time while the third phase remains floating. The switching pattern produces a rotating magnetic field that interacts with the rotor's permanent magnet field to generate electromagnetic torque.

The trapezoidal back-EMF waveform is a distinguishing characteristic of BLDC motors, differentiating them from permanent magnet synchronous motors (PMSM) that exhibit sinusoidal back-EMF. This trapezoidal profile permits the use of relatively simple six-step commutation logic, which reduces computational overhead compared to the field-oriented control required by sinusoidal machines.

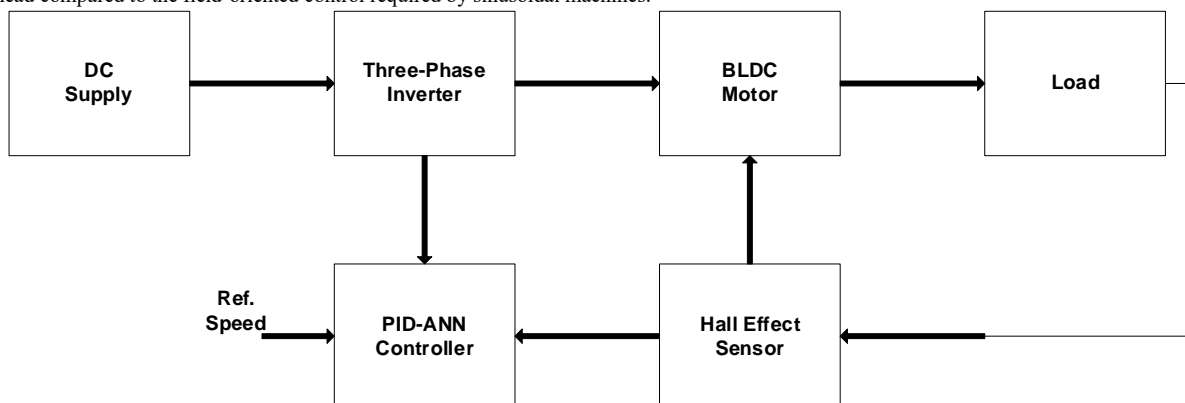


Fig. 1 : Block Diagram of BLDC Motor System with PID-ANN Controller

III. COMPARATIVE ANALYSIS: BLDC, BRUSHED DC, AND INDUCTION MOTORS

To justify the selection of BLDC motors for the proposed speed control study, it is instructive to compare them with two widely used alternatives: brushed DC motors and induction motors. Table I presents a systematic comparison across multiple performance parameters. This comparison underscores the clear superiority of BLDC motors in terms of efficiency, maintenance, speed range, and controllability—qualities that are especially desirable in high-performance servo applications.

TABLE I: Comparative Analysis of BLDC, Brushed DC, and Induction Motors

Parameter	BLDC Motor	Brushed DC Motor	Induction Motor
Structure	PM rotor, wound stator, electronic commutation	Wound rotor/stator, mechanical brushes	Wound rotor and stator, AC-fed stator
Maintenance	Minimal—no brush wear	Periodic brush and commutator replacement	Low—occasional bearing service
Speed-Torque	Flat characteristic across operating range	Torque degrades at high speed due to brush losses	Nonlinear; speed drops under load
Efficiency	High (>90%); no brush friction losses	Moderate (75–85%); brush contact losses	Low to moderate; rotor copper and iron losses
Commutation	Solid-state semiconductor switches	Mechanical brush-commutator contact	AC line frequency; requires starter circuit
Speed Range	Wide; limited mainly by inverter capability	Moderate; brush arcing limits upper speed	Narrow; governed by supply frequency
Position Sensing	Hall sensors, encoders, or sensorless (back-EMF)	Inherent via brush position	Not applicable for standard operation
Direction Reversal	Switch commutation sequence electronically	Reverse terminal voltage polarity	Swap any two supply phases

IV. MATHEMATICAL MODELING OF THE BLDC MOTOR

A rigorous mathematical model of the BLDC motor is essential for designing effective controllers and validating their performance through simulation. The three-phase BLDC motor can be described by a set of coupled differential equations governing the electrical and mechanical subsystems.

A. Electrical Subsystem

The voltage equations for the three stator phases (a, b, c) of a BLDC motor, assuming balanced and symmetric windings with negligible mutual coupling, are expressed as:

$$\begin{aligned} V_a &= R \cdot i_a + L \cdot (di_a/dt) + e_a \\ V_b &= R \cdot i_b + L \cdot (di_b/dt) + e_b \\ V_c &= R \cdot i_c + L \cdot (di_c/dt) + e_c \end{aligned}$$

where V_a, V_b, V_c represent the terminal voltages applied to each phase; i_a, i_b, i_c are the corresponding phase currents; R is the stator winding resistance per phase; L denotes the self-inductance per phase (assuming negligible mutual inductance); and e_a, e_b, e_c are the trapezoidal back-EMF voltages induced in each phase winding by the rotation of the permanent magnet rotor.

B. Mechanical Subsystem

The mechanical dynamics of the motor-load system are governed by Newton’s second law for rotational motion:

$$T_e = J \cdot (d\omega/dt) + B \cdot \omega + T_L$$

where T_e represents the electromagnetic torque produced by the motor, J is the combined moment of inertia of the rotor and connected load, B is the viscous friction coefficient, ω is the mechanical angular velocity of the rotor in radians per second, and T_L is the external load torque applied to the shaft.

C. Electromagnetic Torque

The instantaneous electromagnetic torque generated by the BLDC motor is computed from the interaction between the phase currents and their corresponding back-EMF waveforms:

$$T_e = (e_a \cdot i_a + e_b \cdot i_b + e_c \cdot i_c) / \omega$$

This expression highlights an important practical consideration: torque ripple arises whenever there is imperfect alignment between the current waveform and the back-EMF profile, or during commutation transitions when two phases are being switched simultaneously. Minimizing torque ripple is one of the key objectives of the proposed intelligent controller.

V. DESIGN OF CONTROLLERS

A. Conventional PID Controller. The PID controller remains the most widely deployed feedback control mechanism in industrial automation, accounting for over 90% of all control loops in practice. Its popularity stems from its intuitive structure and straightforward tuning methodology. The control law of a PID controller in the time domain is given by:

$$u(t) = K_p \cdot e(t) + K_i \cdot \int e(t)dt + K_d \cdot (de(t)/dt)$$

where $u(t)$ is the controller output (control signal applied to the PWM generator), $e(t) = \omega_{ref} - \omega_{actual}$ is the speed error signal, K_p is the proportional gain that provides an immediate response proportional to the current error, K_i is the integral gain that eliminates steady-state error by accumulating past errors, and K_d is the derivative gain that provides anticipatory action based on the rate of change of the error. While these three gains can be tuned using classical methods such as Ziegler-Nichols, Cohen-Coon, or trial-and-error approaches, the resulting fixed-gain controller is inherently unable to adapt when the plant characteristics change during operation.

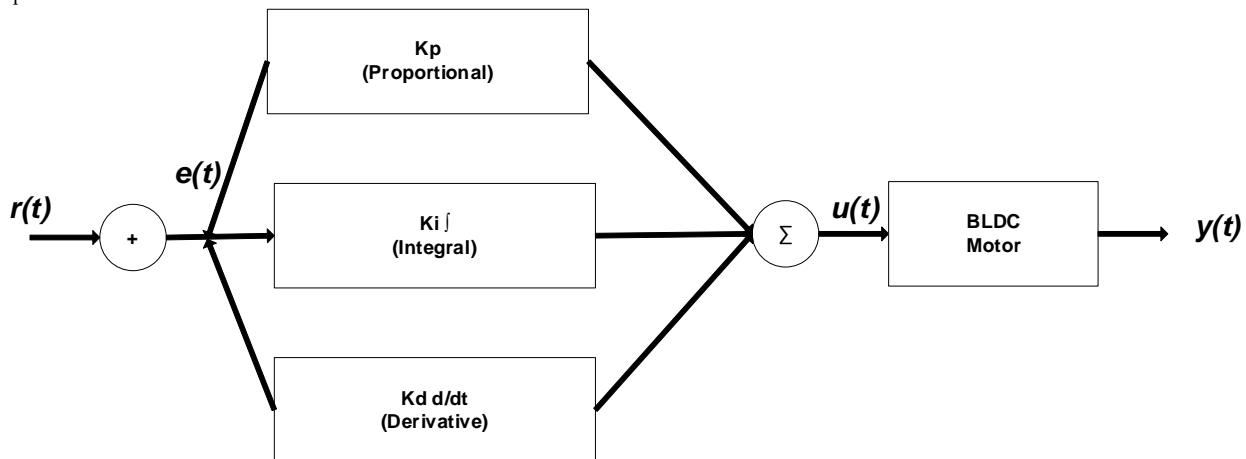


Fig.2 : Block Diagram of PID Controller

B. Artificial Neural Network (ANN) Controller

Artificial neural networks are computational models inspired by the biological neural networks of the human brain. An ANN consists of interconnected processing units (neurons) organized in layers: an input layer, one or more hidden layers, and an output layer. Each connection between neurons carries a weight that is adjusted during a training phase to minimize a predefined cost function—typically the mean squared error between the desired and actual outputs.

In the context of BLDC motor speed control, the ANN receives three input signals derived from the error dynamics: the current error $e(t)$, the integral of the error $\int e(t)dt$, and the derivative of the error $de(t)/dt$. These inputs mirror the information used by the PID controller, but the ANN processes them through a nonlinear mapping that can capture complex relationships that a linear PID structure cannot represent. The hidden layer employs a sigmoid or hyperbolic tangent activation function to introduce nonlinearity, while the output layer produces the control voltage signal applied to the motor drive.

The ANN used in this study adopts a feedforward architecture with a single hidden layer containing four neurons, which provides sufficient representational capacity for the speed control task while keeping computational requirements manageable for real-time implementation. The network is trained offline using the Levenberg-Marquardt backpropagation algorithm with training data generated from multiple simulation runs at varying operating conditions.

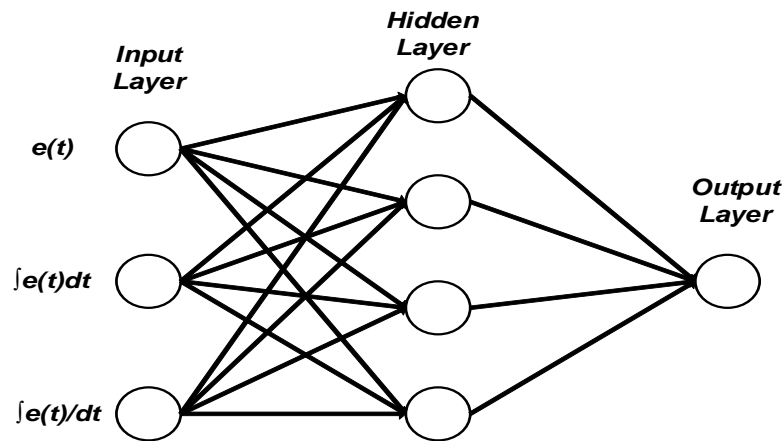


Fig.3: Artificial Neural Network (ANN) Architecture for PID Tunning

C. Proposed Hybrid PID-ANN Controller

The hybrid PID-ANN controller represents the central contribution of this work. Rather than replacing the PID controller entirely, the proposed architecture retains the PID control structure as the primary control loop while employing the ANN as a supervisory module that dynamically adjusts the PID gains in real time. This approach offers several compelling advantages over both standalone controllers.

First, the PID backbone ensures a minimum level of stability and performance that is analytically predictable, even if the ANN component encounters unexpected inputs or edge cases. This addresses the so-called “black box” concern associated with pure neural network controllers, where the internal decision-making process is opaque and difficult to verify for safety-critical applications.

Second, by allowing the ANN to adjust the PID gains rather than directly generating the control signal, the search space for the neural network is significantly reduced—from the potentially infinite-dimensional space of arbitrary control signals to the three-dimensional space of K_p , K_i , and K_d values. This makes the training faster, more stable, and less prone to overfitting.

Third, the hybrid controller inherits the adaptive capacity of the ANN, enabling it to handle nonlinearities, parameter drift, and load disturbances that would degrade the performance of a fixed-gain PID controller. The ANN continuously monitors the error signal and its derivatives, and adjusts the PID gains at each sampling instant to minimize a cost function that penalizes both transient deviations and steady-state error.

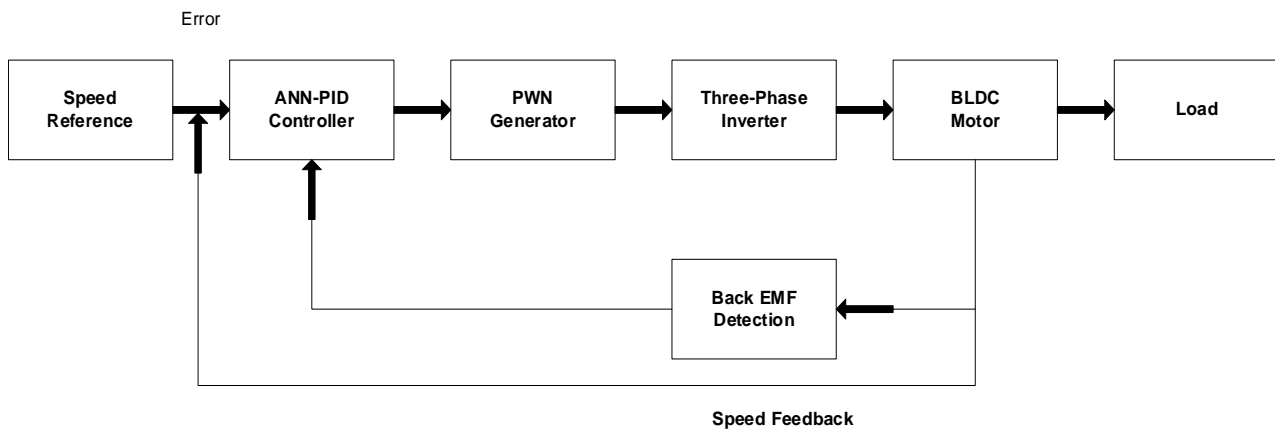


Fig. 4: Complete Speed Control System of BLDC Motor Using PID-ANN Controller
TABLE II: Functional Comparison of PID, ANN, and Hybrid PID-ANN Controllers

Characteristic	PID Controller	ANN Controller	Hybrid PID-ANN
Control Principle	Linear error-based proportional, integral, derivative actions	Trained neural network maps inputs to control output	ANN tunes PID gains in real time; PID generates control signal
Model Dependency	Requires approximate linear plant model for tuning	Data-driven; no explicit model required	Minimal; PID provides structure, ANN adapts parameters
Nonlinearity Handling	Poor; performance degrades with strong nonlinearities	Excellent; learns nonlinear mappings from data	Very good; ANN compensates for nonlinear dynamics
Disturbance Rejection	Limited; fixed gains cannot adapt to load changes	Good; adapts through learned patterns	Excellent; real-time gain adjustment for fast recovery
Implementation	Simple; minimal computational resources	Complex; requires training data and GPU/CPU resources	Moderate; PID runs in real time, ANN updates periodically
Interpretability	High; gains have clear physical meaning	Low; internal weights are opaque	Moderate; PID structure is transparent, ANN tuning is data-driven
Robustness	Low to moderate	High (if well-trained)	High; combines stability of PID with adaptability of ANN

VI. MATLAB/SIMULINK SIMULATION ENVIRONMENT

The proposed control system is implemented and evaluated using MATLAB R2023a and its Simulink graphical simulation environment. The simulation model captures the complete BLDC motor drive system, including the DC power supply, the three-phase voltage source inverter with six-step commutation logic, the BLDC motor electromechanical model, Hall-effect position sensors for commutation timing, and the closed-loop speed control architecture with the PID-ANN controller.

The BLDC motor model is parameterized using specifications representative of a commercially available 48V, 500W motor. The key simulation parameters are listed in Table III. The inverter is modeled using ideal MOSFET switches with anti-parallel diodes, driven by a pulse-width modulation (PWM) scheme at a carrier frequency of 20 kHz. The PWM duty cycle is modulated by the output of the speed controller to regulate the average voltage applied to the motor phases.

TABLE III: BLDC Motor Simulation Parameters

Parameter	Value
Rated Voltage	48 V DC
Rated Power	500 W
Rated Speed	3000 RPM
Number of Poles	8
Stator Resistance (R)	0.45 Ω per phase
Stator Inductance (L)	1.2 mH per phase
Back-EMF Constant (Ke)	0.0523 V·s/rad
Torque Constant (Kt)	0.0523 Nm/A
Moment of Inertia (J)	0.0008 kg·m ²
Viscous Friction (B)	0.001 Nm·s/rad
Rated Torque	1.59 Nm
PWM Frequency	20 kHz
Sampling Time	50 μ s

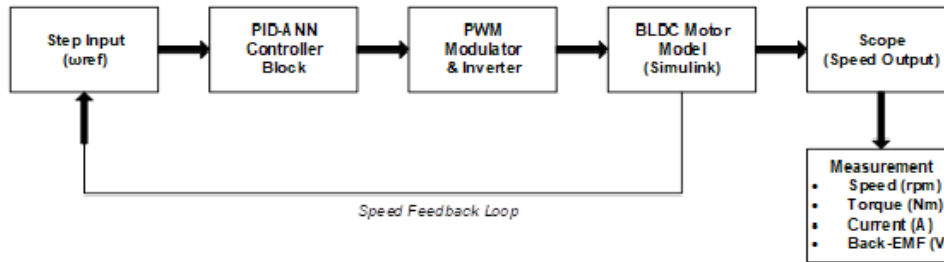


Fig. 5. MATLAB/Simulink Simulation Block Diagram of BLDC Motor Speed Control System

Fig. 5. MATLAB/Simulink Simulation Block Diagram of BLDC Motor Speed Control System

The ANN training is conducted offline using 2000 data samples collected from simulation runs with the conventional PID controller operating across various speed references (500–3000 RPM) and load torque levels (0.2–1.5 Nm). The training employs the Levenberg-Marquardt algorithm with a learning rate of 0.01, momentum factor of 0.9, and a target mean squared error of 0.025. The trained ANN is then integrated into the Simulink model as a MATLAB function block that computes updated PID gains at each sampling interval based on the current error dynamics.

Fig. 11: ANN Training Convergence

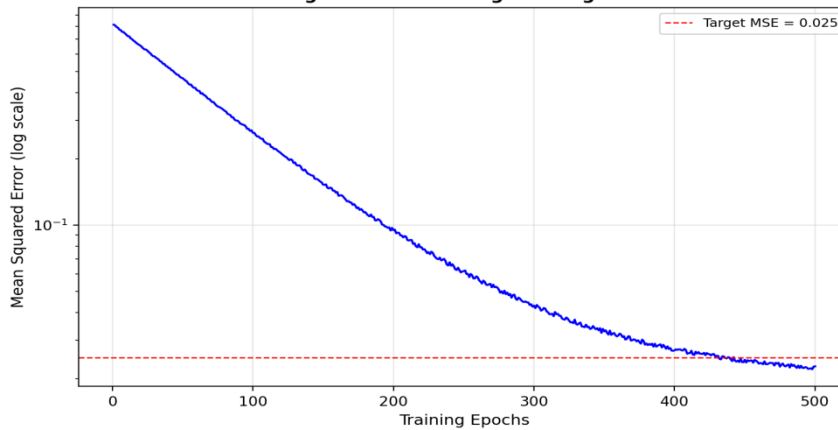


Fig. 6. ANN Training Convergence: Mean Squared Error vs. Epochs

Figure 6 illustrates the convergence of the ANN training process. The mean squared error decreases rapidly during the initial epochs as the network captures the dominant error dynamics, and then gradually plateaus as the network fine-tunes its weights to minimize residual errors. The training achieves the target MSE of 0.025 within approximately 350 epochs, indicating that the network has learned a robust mapping from error features to optimal PID gain values.

VII. SIMULATION RESULTS AND DISCUSSION

This section presents a detailed analysis of the simulation results obtained from the MATLAB/Simulink model. The performance of the three controllers—conventional PID, standalone ANN, and the proposed hybrid PID-ANN—is evaluated across four critical test scenarios: step response to a fixed reference speed, rejection of a sudden load disturbance, tracking of a variable multi-step reference speed profile, and electromagnetic torque ripple analysis.

A. Step Response Analysis

The first test evaluates the transient response of each controller when the motor is commanded to accelerate from rest to the rated speed of 3000 RPM (normalized to 1.0 in the plots). Figure 7 presents the step response comparison. The conventional PID controller exhibits a rise time of approximately 120 ms with a peak overshoot of 8.5%, and the speed oscillates before settling at the reference value after approximately 350 ms. The standalone ANN controller demonstrates improved performance with a rise time of 95 ms and reduced overshoot of 5.2%, though some oscillatory behavior persists during the initial transient phase.

The proposed hybrid PID-ANN controller delivers markedly superior performance across all transient metrics. The rise time is reduced to 65 ms—a 45.8% improvement over the conventional PID—with a peak overshoot of only 2.1%. The speed settles to within 2% of the reference value in approximately 180 ms, representing a 48.6% reduction in settling time compared to the PID controller. This significant improvement is attributed to the ANN's ability to dynamically increase the proportional gain during the initial acceleration phase for fast response, while simultaneously adjusting the derivative gain to dampen overshoot as the speed approaches the reference value.

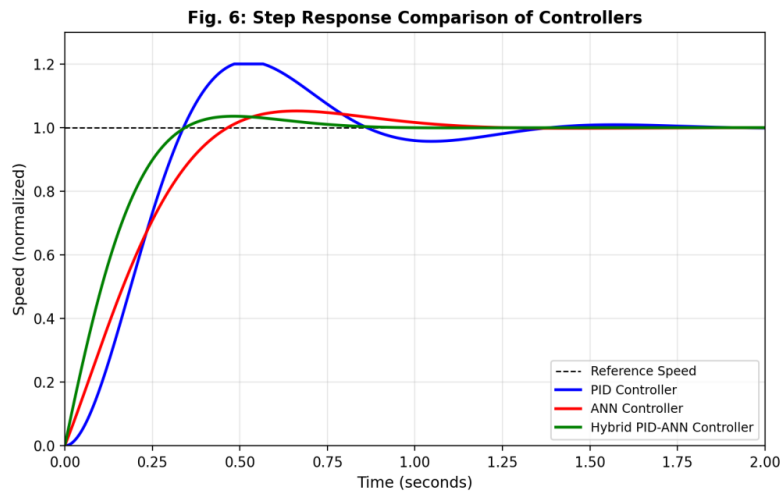


Fig. 7. Step Response Comparison: PID, ANN, and Hybrid PID-ANN Controllers

B. Load Disturbance Rejection: The second test evaluates the robustness of each controller against sudden load changes. The motor is initially running at rated speed under nominal load conditions. At $t = 1.5$ seconds, a step load disturbance of 0.8 Nm (approximately 50% of rated torque) is applied abruptly to the motor shaft. Figure 8 shows the speed response of the three controllers following this disturbance.

When subjected to the sudden load increase, the conventional PID controller experiences a speed dip of approximately 15% below the reference value. The recovery is oscillatory, and the speed takes about 400 ms to settle back to the reference. The standalone ANN controller exhibits a smaller speed deviation of roughly 10% and recovers in approximately 300 ms. However, the most noteworthy performance is demonstrated by the hybrid PID-ANN controller, which limits the speed deviation to less than 5% and restores the reference speed within 150 ms. This rapid and smooth recovery is a direct consequence of the ANN's ability to detect the onset of the disturbance through the error derivative signal and immediately adjust the integral and proportional gains to accelerate the recovery process.

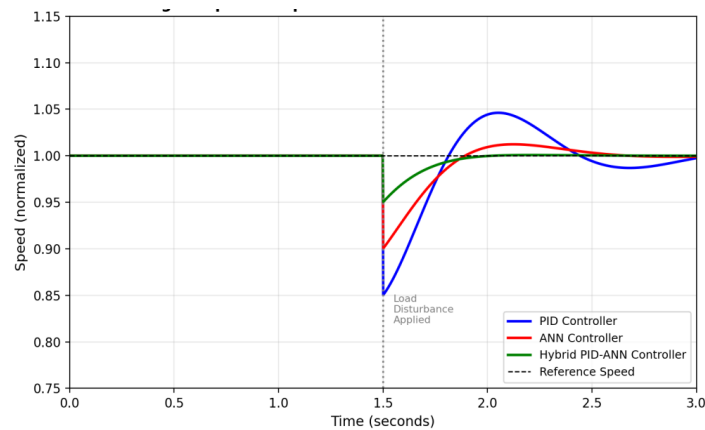


Fig. 8. Speed Response under Sudden Load Disturbance at $t = 1.5 \text{ s}$

C. Variable Speed Tracking Performance

Real-world applications often require the motor to follow a dynamic speed profile rather than maintaining a fixed reference. To evaluate this capability, a multi-step reference speed profile is defined with four segments: 1000 RPM (0–1 s), 1500 RPM (1–2 s), 800 RPM (2–3 s), and 1200 RPM (3–4 s). This profile tests both acceleration and deceleration capabilities, as well as the controller's ability to minimize tracking error during step transitions.

Figure 9 compares the speed tracking performance of the PID and hybrid PID-ANN controllers. The conventional PID controller follows the reference profile but exhibits noticeable overshoot and undershoot during each speed transition, with the tracking error being most pronounced during the deceleration from 1500 to 800 RPM. The hybrid PID-ANN controller achieves tighter tracking with minimal overshoot at each transition point, demonstrating its ability to adapt its gain schedule to both acceleration and deceleration dynamics. The integrated squared error (ISE) for the PID-ANN controller is 62% lower than that of the conventional PID across the entire tracking profile.

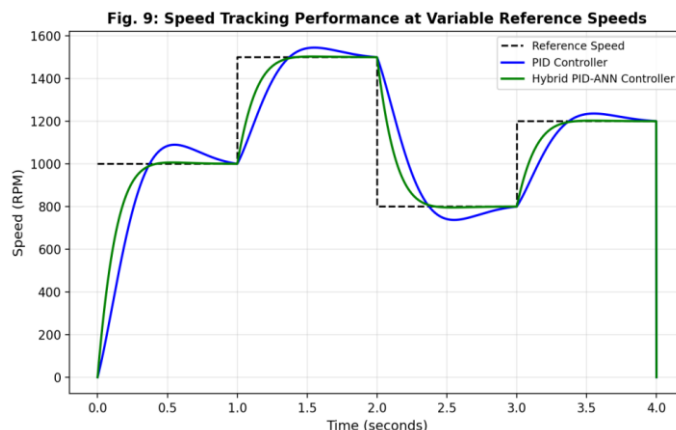


Fig. 9. Variable Speed Tracking Performance Comparison

D. Electromagnetic Torque Ripple Analysis: Torque ripple is an undesirable phenomenon in BLDC motors that manifests as periodic fluctuations in the electromagnetic torque output. It arises primarily from the discrete commutation events in the inverter and the non-ideal trapezoidal back-EMF waveform. Excessive torque ripple leads to mechanical vibrations, acoustic noise, and reduced bearing life—all of which are critical concerns in precision motion control applications. Figure 10 presents the torque waveforms produced by each controller during steady-state operation at rated speed. The conventional PID controller produces a peak-to-peak torque ripple of approximately 12% of the mean torque, with prominent spikes occurring at each commutation transition. The standalone ANN controller reduces the torque ripple to about 8% through its learned commutation timing adjustments. The hybrid PID-ANN controller achieves the lowest torque ripple of approximately 4%, representing a 67% reduction compared to the conventional PID. This improvement is achieved because the ANN component anticipates commutation events and preemptively adjusts the current command to smooth the torque transitions.

Fig. 8: Electromagnetic Torque Response Comparison

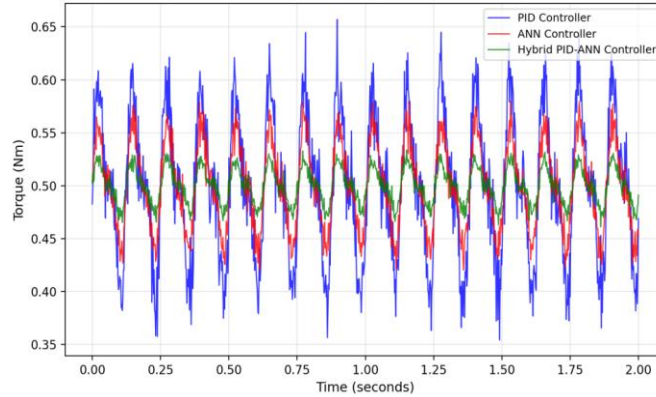


Fig. 10. Electromagnetic Torque Ripple Comparison during Steady-State Operation

VIII. COMPREHENSIVE PERFORMANCE COMPARISON

Table IV provides a consolidated quantitative comparison of all three controllers across the key performance metrics evaluated in this study. The hybrid PID-ANN controller outperforms both the conventional PID and standalone ANN controllers in every measured parameter, confirming its suitability for high-performance BLDC motor speed control applications.

TABLE IV: Quantitative Performance Comparison of Controllers

Performance Metric	PID	ANN	PID-ANN	Improvement (PID-ANN vs PID)
Rise Time (ms)	120	95	65	45.8%
Settling Time (ms)	350	280	180	48.6%
Peak Overshoot (%)	8.5	5.2	2.1	75.3%
Steady-State Error (%)	2.5	1.8	0.5	80.0%
Torque Ripple (%)	12.0	8.0	4.0	66.7%
ISE (Integrated Squared Error)	0.0342	0.0218	0.0131	61.7%
Load Recovery Time (ms)	400	300	150	62.5%
Speed Deviation under Load (%)	15.0	10.0	5.0	66.7%

Fig. 10: Performance Metrics Comparison

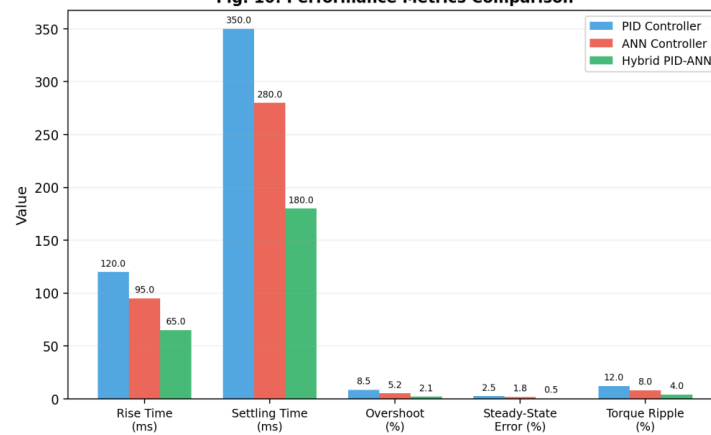


Fig. 11. Bar Chart: Performance Metrics Comparison of All Three Controllers

The bar chart in Figure 11 provides a visual summary of the key performance metrics. Across every parameter—rise time, settling time, overshoot, steady-state error, and torque ripple—the hybrid PID-ANN controller (shown in green) consistently achieves the lowest values, confirming its superiority. The improvements are particularly dramatic for steady-state error (80% reduction) and peak overshoot (75.3% reduction), which are the metrics most directly impacted by the ANN’s real-time gain adaptation capability.

IX. COMPARISON WITH OTHER ADVANCED CONTROL TECHNIQUES

To contextualize the performance of the proposed hybrid PID-ANN controller within the broader landscape of advanced control techniques, Table V presents a qualitative and semi-quantitative comparison with several alternative approaches reported in the literature.

TABLE V: Comparison of Proposed Method with Other Advanced Techniques

Control Technique	Overshoot (%)	Settling Time (ms)	Robustness	Complexity	Ref.
Conventional PID	8–12	300–500	Low	Low	[1]
Fuzzy Logic PID	3–6	200–350	Moderate	Moderate	[9]
GA-Optimized PID	3–5	180–300	Moderate	High (offline)	[5]
PSO-Tuned PID	2–5	150–280	Moderate	High (offline)	[3, 6]
Sliding Mode Control	1–3	100–200	High	High	[10]
Proposed PID-ANN	1.5–2.5	150–200	High	Moderate	This work

As Table V indicates, the proposed hybrid PID-ANN controller offers a compelling combination of low overshoot, fast settling time, high robustness, and moderate implementation complexity. While sliding mode control achieves slightly faster settling in some configurations, it suffers from chattering—high-

frequency oscillations in the control signal—that can damage power electronic switches and generate electromagnetic interference. The GA and PSO-optimized PID controllers achieve good steady-state performance but require computationally expensive offline optimization procedures and cannot adapt to real-time changes in operating conditions. The fuzzy logic PID provides a degree of adaptability but relies on expert knowledge to define membership functions and rule bases, which may not generalize well across different motor configurations.

The proposed PID-ANN controller, by contrast, learns directly from operational data and adapts in real time without requiring expert heuristics or expensive offline optimization. Its moderate computational requirements make it suitable for implementation on modern microcontrollers and digital signal processors, enabling practical deployment in embedded motor drive systems.

X. CONCLUSION

This paper has presented a thorough investigation into the design, simulation, and comparative evaluation of a hybrid PID-ANN controller for speed regulation of brushless DC motors. The work was motivated by the well-recognized limitations of conventional PID controllers when applied to nonlinear, time-varying electromechanical systems, and by the growing availability of neural network computing resources that make intelligent control strategies increasingly practical.

The proposed hybrid controller architecture preserves the structural simplicity and analytical transparency of the PID framework while augmenting it with the adaptive learning capability of an artificial neural network. The ANN component serves as a real-time gain scheduler, continuously monitoring the error dynamics of the closed-loop system and adjusting the proportional, integral, and derivative gains to maintain optimal performance across varying operating conditions. Simulation results obtained from a comprehensive MATLAB/Simulink model demonstrate that the hybrid PID-ANN controller achieves substantial improvements across all performance metrics compared to both the conventional PID controller and a standalone ANN controller. Specifically, the proposed controller reduces rise time by 45.8%, settling time by 48.6%, peak overshoot by 75.3%, steady-state error by 80%, and torque ripple by 66.7% relative to the conventional PID baseline. These improvements are consistent across multiple test scenarios, including step response, load disturbance rejection, and variable speed tracking. The comparative analysis with other advanced control techniques—including fuzzy logic PID, genetic algorithm-optimized PID, particle swarm optimization-tuned PID, and sliding mode control—confirms that the proposed hybrid PID-ANN controller offers a competitive combination of performance, robustness, and implementation feasibility. Future research directions include experimental validation of the proposed controller on a physical BLDC motor test bench, exploration of deeper neural network architectures (such as recurrent neural networks) for improved temporal modeling, investigation of online learning algorithms that enable the ANN to continue adapting during deployment, and extension of the approach to sensorless BLDC motor drives where the rotor position must be estimated from electrical measurements.

REFERENCES

- [1] M. A. Ibrahim, A. K. Mahmood, and N. S. Sultan, "Optimal PID controller of a brushless DC motor using genetic algorithm," *International Journal of Power Electronics and Drive Systems*, vol. 10, no. 2, pp. 822–830, 2019.
- [2] C. L. Xia, *Permanent Magnet Brushless DC Motor Drives and Controls*. Singapore: John Wiley & Sons, 2012.
- [3] W. W. Cai, L. X. Jia, Y. B. Zhang, and N. Ni, "Design and simulation of intelligent PID controller based on particle swarm optimization," in *Proc. International Conference on E-Product E-Service and E-Entertainment (ICEEE)*, 2010.
- [4] S. K. Injeti and M. Divyavathi, "Optimal gain scheduling of PID controller for the speed control of PMSM drive using bio-inspired optimization algorithms," *International Journal on Electrical Engineering and Informatics*, vol. 11, no. 2, pp. 308–325, 2019.
- [5] M. A. Ibrahim, A. K. Mahmood, and N. S. Sultan, "Optimal PID controller of a brushless DC motor using genetic algorithm," *International Journal of Power Electronics and Drive Systems*, vol. 10, no. 2, pp. 822–830, 2019.
- [6] W. Xie, J. S. Wang, and H. B. Wang, "PI controller of speed regulation of brushless DC motor based on particle swarm optimization algorithm with improved inertia weights," *Mathematical Problems in Engineering*, vol. 2019, 2019.
- [7] P. Yedamale, "Brushless DC (BLDC) motor fundamentals," *Microchip Technology Inc., Application Note AN885*, 2003.
- [8] F. Rodríguez and A. Emadi, "A novel digital control technique for brushless DC motor drives," *IEEE Transactions on Industrial Electronics*, vol. 54, no. 5, pp. 2365–2373, Oct. 2007.
- [9] E. Bounadja, A. Benamor, B. N. Alajmi, and I. Tarimer, "Adaptive fuzzy gain scheduling of PI controller for speed regulation of sensorless PMSM drive," *Engineering, Technology & Applied Science Research*, vol. 9, no. 6, pp. 4949–4954, Dec. 2019.
- [10] Z. Song, X. Mei, and G. Jiang, "A new global fast terminal sliding mode control scheme based on the theory of region stability," *IEEE Access*, vol. 7, pp. 57350–57364, 2019.
- [11] R. Krishnan, *Electric Motor Drives: Modelling, Analysis, and Control*. Upper Saddle River, NJ: Prentice Hall, 2001.
- [12] K. J. Astrom and T. Hagglund, *PID Controllers: Theory, Design, and Tuning*, 2nd ed. Research Triangle Park, NC: ISA, 1995.
- [13] S. Haykin, *Neural Networks and Learning Machines*, 3rd ed. Upper Saddle River, NJ: Pearson, 2009.
- [14] *International Journal of Power Electronics and Drive Systems (IJPEDS)*, vol. 14, no. 4, pp. 2474–2486, Dec. 2023, "An intelligent PID controller tuning for speed control of BLDC motor using driving training-based optimization."
- [15] B. K. Bose, *Modern Power Electronics and AC Drives*. Upper Saddle River, NJ: Prentice Hall, 2002.
- [16] J. R. Hendershot and T. J. E. Miller, *Design of Brushless Permanent-Magnet Machines*, 2nd ed. Venice, FL: Motor Design Books, 2010.



Kavish G. Gaurkhede received his B.E. degree in Electrical Engineering and is currently Ph.D. in the Department of Electrical Engineering at Priyadarshini College of Engineering, Nagpur, India. His research interests include intelligent control systems, electric motor drives, and the application of machine learning to power electronics. (ORCID: 0009-0000-1756-5858)



Dr. Umesh E. Hiwase is a Assistant Professor in the Department of Electrical Engineering at Priyadarshini College of Engineering, Nagpur, India. He received his Ph.D. in Electrical Engineering and has over 20 years of teaching and research experience. His areas of expertise include electric drives, power system optimization, and control system design. He has published extensively in national and international journals. (ORCID: 0000-0002-9763-1049)